Incompressible Flow in Conical Contractions Using the Method of Integral Relations

S. G. LIDDLE*
General Motors Research Laboratories, Warren, Mich.

AND

R. D. ARCHER†

University of New South Wales, Sydney, Australia

The method of integral relations is used to solve the inviscid incompressible flowfield in contractions of arbitrary shape. Theoretical velocity fields for four conical contractions are presented. The theoretical wall pressures for these four shapes agree well with experimental values obtained by using water as the working fluid.

Nomenclature

F = dimensionless flow rate [Eqs. (16, Al.7, A2.10)]
P = pressure
r,z = cylindrical, or cartesian coordinate (Fig. 1)
R = radius of curvature (Table 1)
u,w = cylindrical, or cartesian, velocity components
V = local velocity
ρ = fluid density
θ = conical angle of contraction (Table 1)

Superscript

n = 0 in plane flow (= 1-in. axisymmetric flow)

Subscripts

i,j = boundary of strip i in field of j strips (Fig. 1)
0 = stagnation value

Introduction

THE design and analysis of contractions, whether a simple area change in a pipe, or part of a nozzle or venturi, is often based on the assumption of one-dimensional flow (e.g., Ref. 1, Chap. 3). For contractions characterized by small included angles and large radii of curvature, this may well be satisfactory. However, as the contraction angles become steeper and the radii shorter, appreciable errors appear.

Unlike previous attempts to obtain a higher-order flowfield solution, this paper attempts to solve the problem directly given only an arbitrary wall shape. The wall shape to be considered here is described by straight lines and circles and is typical of simple contractions as found, e.g., in pipes and venturis. The study reported here is part of a complete flowfield solution[6] including inviscid compressible flow in nozzles of arbitrary shape.

The method of integral relations[2-5] is used to solve the partial differential equations of motion, by making approximations to reduce them to a system of simultaneous ordinary differential equations for integration by standard numerical techniques.

The method has only been applied here to the incompressible flow in axisymmetric contractions but the equations have been written to include the plane flow case.

A cylindrical or cartesian coordinate system was chosen and is shown in Fig. 1. The geometry shown in Fig. 1 and Table 1 is found in simple rocket nozzles and was that used in the wider study mentioned previously.[6]

In applying the method of integral relations, the flowfield was divided into longitudinal strips. Figure 1 shows a two-strip field. Further, to generalise the discussion for an arbitrary number of strips j, the values of parameters at the strip boundaries were designated by a double subscript wherein the first subscript i defines the particular boundary in the field of j strips. Thus, the centerline is always given by $i = 0$, and the wall by $i = j$. Intermediate lines will have integer values of i between 0 and j counted outward from the centerline. This also prevents ambiguity in a context of j strips where w_i by itself has j meanings.

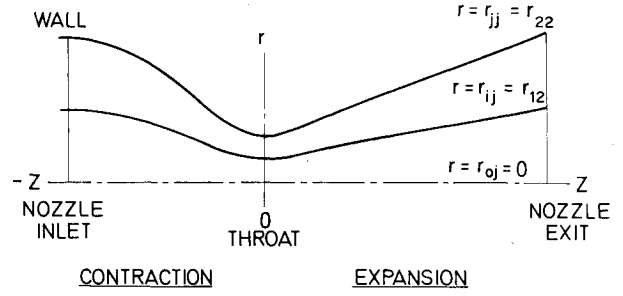

Fig. 1 Nozzle coordinate system and division of flowfield into two strips.

Table 1 Nozzle and contraction geometry (contractions are specified by values of parameter in the order R_c/θ)

NOZZLE No.	R_{inlet}	R_c	R_I	R_{exit}	α	θ	THROAT RADIUS inches
1	2·684	4·000	1·500	2·684	15°	30°	0·750
2	2·684	2·000	1·500	2·684	15°	30°	0·750
3	2·684	2·000	1·500	2·684	15°	45°	0·750
4	2·684	0·625	1·500	2·684	15°	30°	0·750

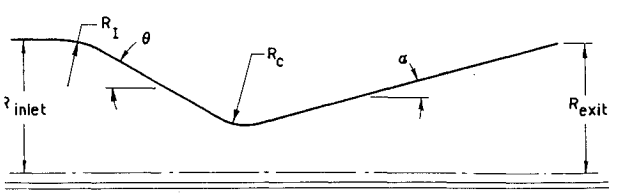

Received June 15, 1970; revision received October 19, 1970.

* Senior Research Engineer, Emissions Research Department. Member AIAA.

† Senior Lecturer, School of Mechanical and Industrial Engineering. Member AIAA.

The general equations for axisymmetric or plane adiabatic flow of an ideal inviscid incompressible fluid are

Continuity

$$\partial ur^n/\partial r + \partial wr^n/\partial z = 0 \tag{1}$$

Irrotationality

$$\partial w/\partial r - \partial u/\partial z = 0 \tag{2}$$

Bernoulli's equation

$$P + \rho V^2/2 = \text{const} \tag{3}$$

These three equations are rendered dimensionless by referring the velocities to the maximum velocity defined by Eq. (4), lengths to the throat radius and the pressure to its stagnation value.

$$V_{\max} = (2P_0/\rho)^{1/2} \tag{4}$$

The form of Eqs. (1) and (2) is not changed by normalization and, from this point on, we take the symbols to mean their normalized values. Equation (3), however, becomes

$$P + V^2 = 1 \tag{5}$$

where again the symbols P and V now mean their normalized values. This algebraic equation is of course only used to find the pressure field given the solution to Eqs. (1) and (2). We note that the two simultaneous partial differential Eqs. (1) and (2) have the "divergence form" recommended for the method of integral relations.[2]

Two boundary conditions are given by flow properties at the wall and centerline. For the flow to follow the wall

$$u_{jj} = w_{jj}dr_{jj}/dz \tag{6}$$

And, taking the centerline as an axis of symmetry and a streamline

$$u_{0j} = 0 \tag{7}$$

Application of the Method of Integral Relations

To illustrate the way in which the method of integral relations is used here, the irrotationality Eq. (2) will be considered for the one strip case.

Generalized equations for an arbitrary number of strips j and particular results for $j = 0$ to 3 are given in Ref. 6.

The boundaries for the one strip case are the centerline ($r = 0$) and the wall ($r = r_{11}$). Equation (2) is integrated with respect to r from $r = 0$ to $r = r_{11}$ with the result

$$w_{11} - w_{01} - \int_0^{r_{11}} \frac{\partial u}{\partial z}\, dr = 0 \tag{8}$$

Applying Liebnitz's Rule to the integral and observing the boundary conditions,

$$w_{11} - w_{01} - d/dz \left(\int_0^{r_{11}} udr\right) + u_{11}\frac{dr_{11}}{dz} = 0 \tag{9}$$

In the general multistrip problem, it is apparent that u is both continuous and bounded in a closed domain. Therefore, by the Weierstrass theorem, u can be uniformly approximated by a polynomial. From symmetry, the polynomial contains only odd powered terms. Therefore, u is taken as

$$u = \sum_{k=1}^{j} [u]_k \left(\frac{r}{r_{jj}}\right)^{2k-1} \tag{10}$$

where the $[u]_k$ terms are functions of the values of u at the strip boundaries and the degree of the polynomial is determined by the chosen number of strips j. For the one strip case, the approximation is

$$u = [u]_1(r/r_{11}) \tag{11}$$

At the wall $u = u_{11}$ and $r = r_{11}$, hence $[u]_1 = u_{11}$ and therefore

$$u = u_{11}(r/r_{11}) \tag{12}$$

Equation (12) is integrated with respect to r from $r = 0$ to $r = r_{11}$ with the result

$$\int_0^{r_{11}} udr = u_{11}\frac{r_{11}}{2} \tag{13}$$

The substitution of Eq. (13) into Eq. (9) transforms it into an ordinary first-order differential equation. The resulting equation can be rewritten, upon applying boundary conditions, in a form suitable for computation

$$dw_{11}/dz = [2w_{11} - 2w_{01} - w_{11}r_{11}d^2r_{11}/dz^2 + w_{11}(dr_{11}/dz)^2]/(r_{11}dr_{11}/dz) \tag{14}$$

Similar treatment of the continuity Eq. (1) provides an Eq. (A1.2) for dw_{01}/dz. However, this time a polynomial approximation is required for w, which must, unlike Eq. (10) for u, be an even function.

The two equations dw_{01}/dz and dw_{11}/dz in the two unknowns w_{01} and w_{11} can now be integrated simultaneously using any appropriate numerical method. Both the Runge-Kutta method and the Adams-Moulton method have been used.

Higher-order approximations can be written in the same manner, thereby offering better accuracy of the method as the number of strips and, hence, the number of terms in the approximation increases.

Advancing from one to two strips, the flowfield was divided by a line located midway between the centerline and the wall ($r_{12} = r_{22}/2$, Fig. 1). Equations (1) and (2) were now integrated first from $r = 0$ to $r = r_{12}$ and then from $r = 0$ to $r = r_{22}$. This gave four ordinary differential equations in four unknown, w_{02}, w_{12}, w_{22}, and u_{12}, which were integrated in the same way as the one strip equations.

The method yields the familiar one-dimensional flow equations, if the zero degree term only is retained in each approximation [e.g., Eq. (10)] for u and w. This makes u zero and w independent of r. The Appendices present the equations for the one and two strip cases in a form ready for use in computation.

To perform the integration, initial and final boundary values must be specified. This was done with the aid of conditions at the entrance and throat of the contraction. At these positions, the slope of the wall $dr_{jj}/dz = 0$. In the one strip case for example, this means first that at these locations the denominator of Eq. (A1.1) is zero. For nonsingular wall velocity gradient, the numerator of dw_{11}/dz must also be zero

$$2w_{11} - 2w_{01} - w_{11}r_{11}d^2r_{11}/dz^2 = 0$$

or

$$w_{01}/w_{11} = 1 - (r_{11}d^2r_{11}/dz^2)/2 \tag{15}$$

At the throat, d^2r_{11}/dz^2 must be either zero or a positive finite quantity. As a result, the wall velocity w_{11} will always be equal to or larger than the centerline velocity w_{01}. In the special case where $d^2r_{11}/dz^2 = 0$, the flow is uniform, $w_{01} = w_{11}$. Secondly, zero wall slope allows Eq. (A1.2) to be integrated. Thus, for one strip, and with $n = 1$

$$(w_{01} + w_{11})r_{11}^2 = F \quad \text{for} \quad (w_{01}/w_{11} + 1)r_{11}^2 = F/w_{11} \tag{16}$$

where F is the dimensionless flow rate in the contraction. It should be observed that, like w_{01}/w_{11}, F/w_{11} depends only on geometry. A reference value of $w_{11} = 1$ at the throat has been used here. Thus, when Eqs. (15) and (16) are written at the throat, the flow rate F can be calculated, and used with the same equations written at the entrance to find initial values of w_{01} and w_{11}. Integration proceeds in a single run from entrance to throat.

The two strip case, however, requires iteration on unknown initial conditions. Following a procedure similar to that pre-

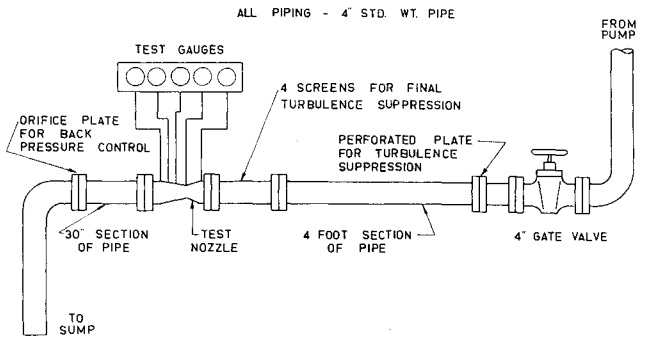

Fig. 2 Water flow test.

vious for the one strip case and using Eq. (A2.1) instead of Eq. (A1.1), two of four undetermined initial values u_{12}, w_{02}, w_{12}, and w_{22} can be obtained. Iteration is required on the other two initial values, say u_{12} and w_{12}. If the assumed values are in error, w_{02} or w_{22} go to zero in the course of the integration.

Integration across discontinuities in wall curvature was found to be possible using sufficiently small step size. The influence on the flowfield in the neighbourhood of such a point appears in some results as discontinuities in velocity contour slope. Although it might be expected that there should be no preferred direction of integration in an elliptic domain, experience indicates that integration in the reverse direction with this method tends to be unstable. A step size of 0.005 has been found to be satisfactory for both stability and accuracy. Interpolation for velocity contours and streamlines used the assumed approximations for velocity and the flow rate F. Typical computing times for a one strip run were 45 sec on an IBM/360 model 50. The two strip case required about 2 min/iteration run and about 10–20 iterations to converge to a satisfactory solution.

In this paper the method has only been applied to axisymmetric conical contractions. Extension to plane contractions requires only that n be put equal to zero in Eq. (1) to obtain the appropriate continuity equation, or in the equations of the Appendices to obtain the integrated equations.

To extend the method to annular nozzles and to those with no axis of symmetry, the only changes are in boundary conditions appropriate to new wall geometry. The lower limit of integration on r takes an arbitrary finite value r_{0j} different from zero, and its presence in the equations increases their complexity.

Integration can readily be carried into the diverging portion of a nozzle. But the validity of the solution can be expected to disappear if separation, or large boundary-layer growth occurs.

Experiment

Four contractions with the proportions presented in Table 1 and a 0.750-in. throat radius were constructed. Tests were conducted in the Hydraulics Laboratory, School of Mechanical and Industrial Engineering, University of New South Wales. The test arrangement is depicted in Fig. 2. Water at a 150-ft head was supplied by a 6-in. centrifugal pump driven by a d.c. motor developing 65 hp. A 4-in. gate valve was used to control the flow rate. A perforated plate immediately downstream of the valve reduced the initial turbulence level of the stream, while a 4-ft length of straight 4-in.-diam pipe followed by four 24-mesh 28-gauge screens were used for final turbulence control. An orifice located 30 in. downstream of the test contraction was used to maintain the test section at pressures high enough to prevent cavitation. The static pressures at 9 or 10 points along the wall were measured using Bourdon tube pressure gauges. The esti-

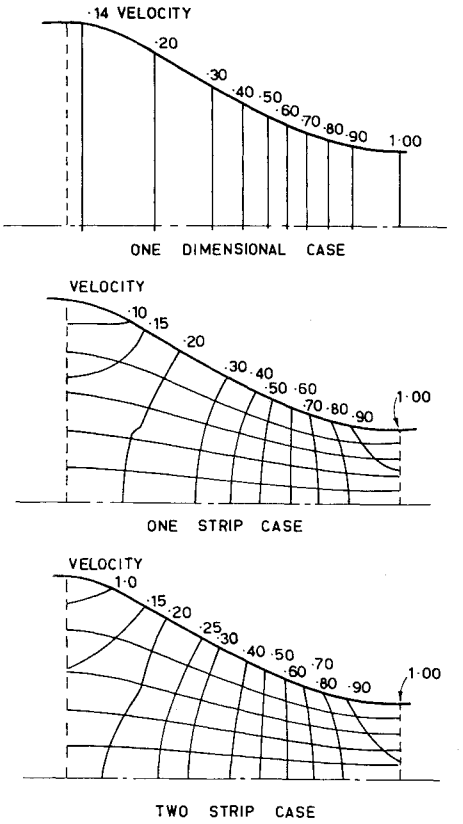

Fig. 3 Velocity field and streamlines for Contraction No. 1 ($R_c = 4.0, \theta = 30°$).

mated total error of the system including instrument and reading errors is 2%. The Reynolds number based on the local diameter was approximately 5×10^3 at the contraction entrance and approximately 1×10^6 at the throat. Small

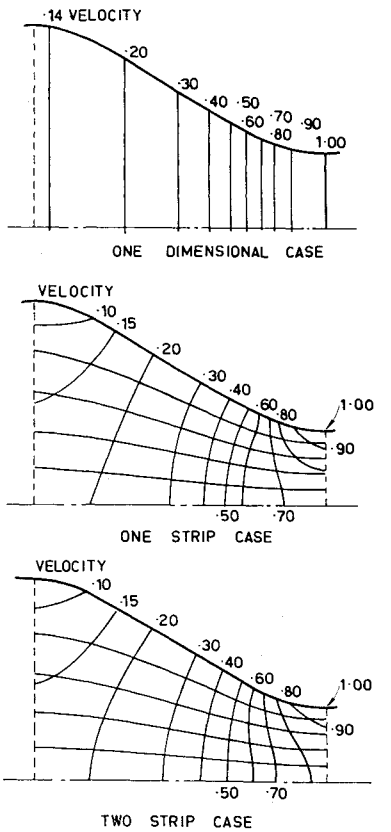

Fig. 4 Velocity field and streamlines for Contraction No. 2 ($R_c = 2.0, \theta = 30°$).

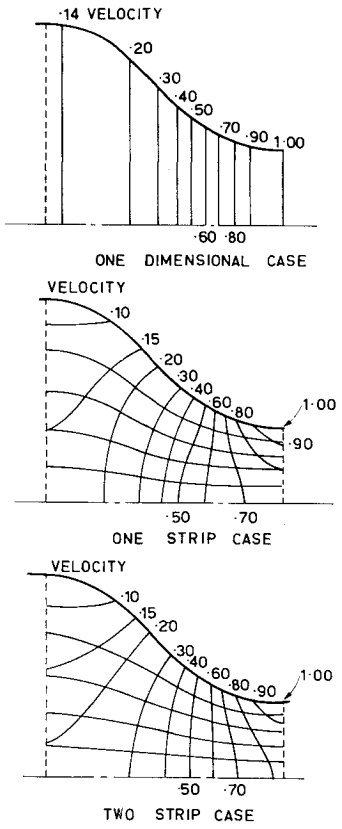

Fig. 5 Velocity field and streamlines for Contraction No. 3 (R_c = 2.0, θ = 45°).

variations in Reynolds number had no significant effect on the pressure distribution.

Discussion of Results

Velocity fields and wall pressure profiles for the four nozzles of Table 1 were computed for the one dimensional, and one and two strip theory. The velocity fields are shown in Figs. 3–6, and wall pressure profiles in Figs. 7–10, together with the experimental results. Separation occurred in the diverging section of all nozzles tested, and experimental results soon departed from the inviscid theory downstream of the throat (Fig. 11).

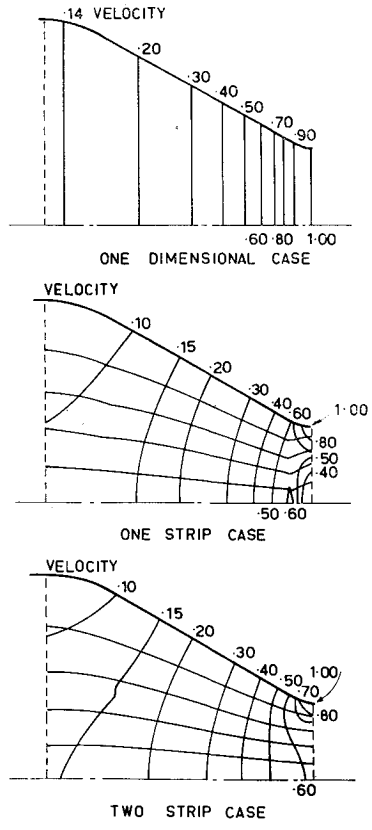

Fig. 6 Velocity field and streamlines for Contraction No. 4 (R_c = 0.625, θ = 30°).

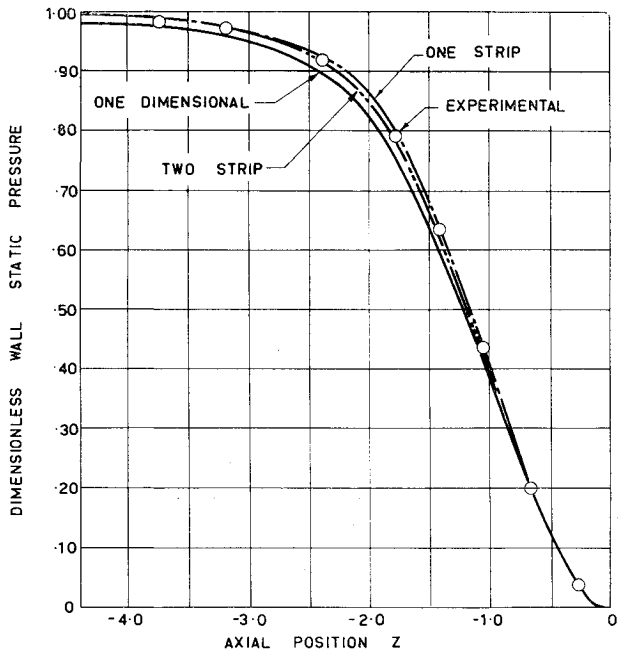

Fig. 7 Dimensionless wall static pressure for Contraction No. 1 (R_c = 4.0, θ = 30°).

For the contractions, the experimental wall pressures show good agreement with the one strip solution in the first two cases, and with the two strip solution in the last two. It is evident that as the contraction angle θ increases and radius of curvature R_c decreases, the difference between the experimental values and the lower-order solutions increases. The two strip solutions show good agreement for all the nozzles, but in the extreme cases (θ = 45° or R_c = 0.625), the flow-fields for the one and two strip solutions show large differences when compared. Thus, a three strip solution is required to

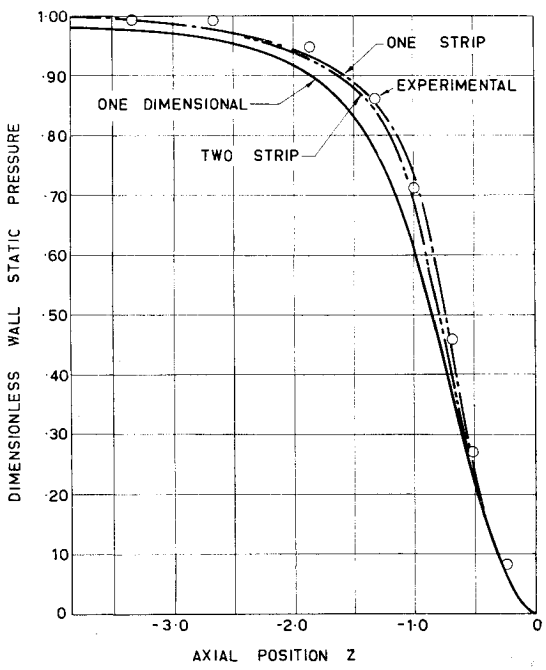

Fig. 8 Dimensionless wall static pressure for Contraction No. 2 (R_c = 2.0, θ = 30°).

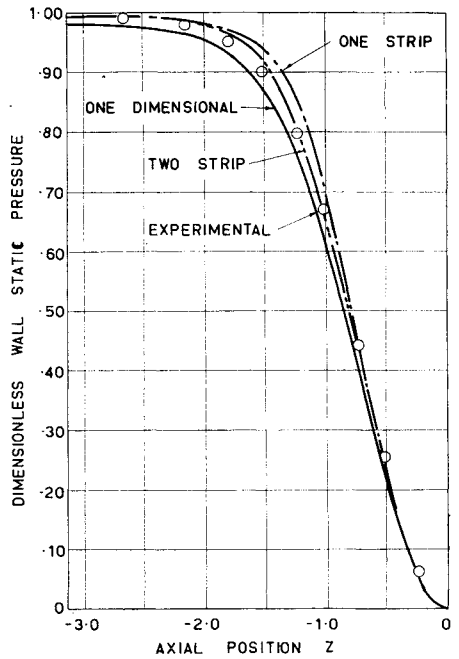

Fig. 9 Dimensionless wall static pressure for Contraction No. 3 ($R_c = 2.0, \theta = 45°$).

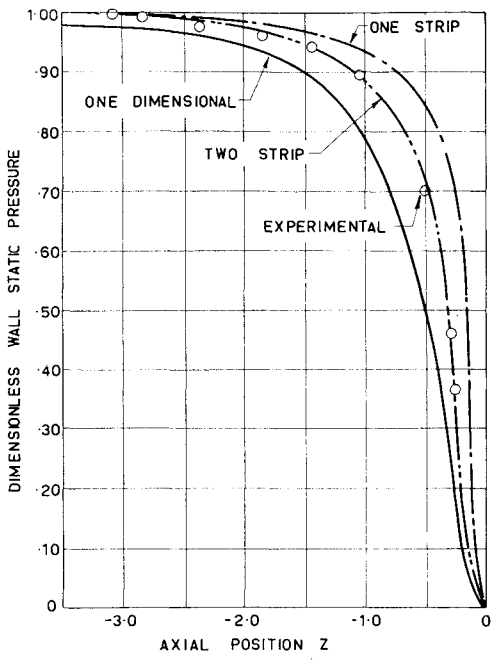

Fig. 10 Dimensionless wall static pressure for Contraction No. 4 ($R_c = 0.625, \theta = 30°$).

demonstrate convergence of the numerical solution. This is, however, a formidable task.

The method as used here cannot give useful results in the parallel pipe upstream of the entrance, because it will merely predict the one-dimensional solution there. Nevertheless, it is interesting to observe in the theoretical velocity fields shown in Figs. 3–6 a low-velocity region adjacent to the wall at the entrance, under the influence of the wall curvature term d^2r_{11}/dz^2 in Eq. (15). Another effect of this term is the high wall velocity at the contraction throat. In the entrance d^2r_{11}/dz^2 is negative, w_{01}/w_{11} is greater than one, and hence wall velocity is low. At the throat w_{01}/w_{11} is less than one, and hence wall velocity is higher than on the axis, and in fact attains the highest value for the whole field there, $w_{11} = 1$. On the other hand, for a contraction designed with local wall curvature zero at both the entrance and exit, a uniform velocity across the entrance or exit plane would be predicted by the solution.

Conclusion

The method of integral relations has been used to determine the inviscid flowfield in axisymmetric contractions of arbitrary shape. The solution for the first-order one strip case is relatively simple to compute but becomes progressively less accurate as contraction angles increase and radii of curvature decrease. For all four geometries studied, the two strip solution was sufficiently accurate for predicted wall pressures but required considerable computer time since initial values had to be found by iteration.

Appendix 1: Incompressible Flow Equations—One Strip

The differential equations from continuity and irrotationality

$$dw_{11}/dz = [2w_{11} - 2w_{01} - w_{11}r_{11}d^2r_{11}/dz^2 + w_{11}(dr_{11}/dz)^2]/(r_{11}d_{11}/dz) \quad \text{(A1.1)}$$

$$dw_{01}/dz = -[w_{01}{}^{(n+1)}dr_{11}/dz]/r_{11} - (4 - n)[w_{11}{}^{(n+1)}dr_{11}/dz]/(8 - 5n)r_{11} - [(4 - n)dw_{11}/dz]/(8 - 5n) \quad \text{(A1.2)}$$

Momentum

$$P_{01} + w_{01}{}^2 = 1 \quad \text{(A1.3)}$$

$$P_{11} + u_{11}{}^2 + w_{11}{}^2 = 1 \quad \text{(A1.4)}$$

Boundary conditions

$$u_{11} = w_{11}dr_{11}/dz \quad \text{(A1.5)}$$

$$u_{01} = 0 \quad \text{(A1.6)}$$

Integrated continuity equation

$$[(8 - 5n)w_{01} + (4 - n)w_{11}]r_{11}{}^{(n+1)} = F \quad \text{(A1.7)}$$

Appendix 2: Incompressible Flow Equations—Two Strips

$$dw_{22}/dz = [14w_{22} - 32w_{12} + 18w_{02} - 16u_{12}(dr_{22}/dz) + 11w_{22}(dr_{22}/dz)^2 - 3r_{22}w_{22}(d^2r_{22}/dz^2)]/3r_{22}(dr_{22}/dz) \quad \text{(A2.1)}$$

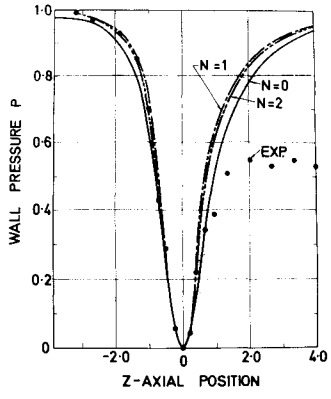

Fig. 11 Comparison of flowfield and wall pressures for Nozzle No. 2.

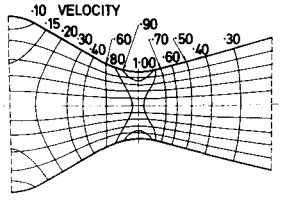

$$du_{12}/dz = [w_{22} + 8w_{12} - 9w_{02} + u_{12}(dr_{22}/dz) + w_{22}(dr_{22}/dz)^2]/3r_{22} \quad (A2.2)$$

$$dw_{02}/dz = (n+1)\{3r_{22}(dw_{22}/dz) + 32w_{12}(dr_{22}/dz) - 64u_{12} - [18w_{02} - 3(n+1)w_{22}]dr_{22}/dz\}/18r_{22} \quad (A2.3)$$

$$dw_{12}/dz = \{-3r_{22}(dw_{22}/dz) + 8(1-3n)[u_{12} - (w_{12}dr_{22}/dz)/2] - (n+1)(12w_{12} + 3w_{22})(dr_{22}/dz)\}/12r_{22} \quad (A2.4)$$

Momentum

$$P_{02} + w_{02}^2 = 1 \quad (A2.5)$$

$$P_{12} + u_{12}^2 + w_{12}^2 = 1 \quad (A2.6)$$

$$P_{22} + w_{22}^2[1 + (dr_{22}/dz)^2] = 1 \quad (A2.7)$$

Boundary conditions

$$u_{22} = w_{22}(dr_{22}/dz) \quad (A2.8)$$

$$u_{02} = 0 \quad (A2.9)$$

The integrated continuity equation between centerline and wall

$$r_{22}^{(n+1)}[(24 - 39n)w_{02} + (128 - 48n)w_{12} + (28 - 3n)w_{22}] = F \quad (A2.10)$$

References

[1] Vennard, J. K., *Elementary Fluid Mechanics*, Wiley, New York, 1954.

[2] Dorodnitsyn, A. A., "Method of the Integral Relations for the Numerical Solution of Partial Differential Equations," Academy of Sciences of the U.S.S.R., Institute of Exact Mechanics and Computing Techniques, Moscow (Transactions TT62-25867, Clearing House for Scientific and Technical Information, U.S. Dept. of Commerce), 1958.

[3] Dorodnitsyn, A. A., "One Method of Numerical Solution of Certain Non-Linear Problems in Aerodynamics," *Vsesofuznyi Matematicheskil Slezd*, Trudy, No. 3, pp. 447–53. [UCRL Trans—993 (L), Sept. 1963, University of California, Berkeley, Lawrence Radiation Lab.].

[4] Belotserkovskii, O. M., "A Numerical Method of Integral Relations," *U.S.S.R. Computational Mathematics and Mathematical Physics*, Vol. 3, No. 5, 1963, pp. 823–58.

[5] Belotserkovskii, O. M., "The Numerical Solution of Problems in Gas Dynamics," *Basic Developments in Fluid Dynamics*, edited by M. Holt, Vol. 1, Academic Press, 1965.

[6] Liddle, S. G., "A Study of Fluid Flow in Nozzles," Ph.D. thesis, 1968, University of New South Wales.